# Experimental Evaluation of Inter-Channel Multi-Phase Mixing Through a Narrow Gap

**James W. Gose**

Department of Naval Architecture and Marine Engineering
University of Michigan
2600 Draper Dr., Ann Arbor, MI 48109, USA
jgose@umich.edu

**Zakaria Tazi Hnyine**

Department of Mechanical Engineering
University of Twente
Drienerlolaan 5, Enschede, 7522 NB, NL
z.tazihnyine@student.utwente.nl

**Simo A. Mäkiharju**

Department of Mechanical Engineering
University of California - Berkeley
6179 Etcheverry Hall, Berkeley, CA 94720, USA
makiharju@berkeley.edu

**Alexander G. Mychkovsky**

Bettis Atomic Power Laboratory
Naval Nuclear Laboratory
West Mifflin, PA 15122, USA
alexander.mychkovsky@unnpp.gov

**John R. Buchanan, Jr**

Bettis Atomic Power Laboratory
Naval Nuclear Laboratory
West Mifflin, PA 15122, USA
jack.buchanan@unnpp.gov

**Kirk T. Lowe**

Bettis Atomic Power Laboratory
Naval Nuclear Laboratory
West Mifflin, PA 15122, USA
kirk.lowe@unnpp.gov

**Steven L. Ceccio**

Department of Naval Architecture and Marine Engineering
University of Michigan
2600 Draper Dr., Ann Arbor, MI 48103, USA
ceccio@umich.edu

## ABSTRACT

Two-phase mass transfer through a narrow gap connecting two adjacent channels was investigated as a function of gap geometry and flow conditions. The vertical test section consisted of two 127 mm × 127 mm channels connected through a 1,219 mm ($L$) × 229 mm ($W$) height-adjustable gap (0-50 mm). The single-phase (water) inlet Reynolds number for each channel was independently varied from $4\times10^4$ to $1\times10^5$. The gross single phase fluid exchange between the flow channels through the connecting gap, or mixing, has been previously characterized. For the two-phase experiments, air was injected to either or both flow channels inlets *via* a needle array to produce nominally monodispersed bubbles with a mean diameter of 5 to15 mm, depending on the air flow rate. The air flow rates were metered at the inlet and varied to achieve a cross-sectional void fraction of 1% to 15%. Multi-phase mixing through the gap was quantified based on the measured mass flow rates of the water and air and through measurement of a liquid dye tracer concentration at the inlet and outlet of each channel. The void fraction, bubble size, and gas phase velocity were measured using dual-plane wire mesh conductivity sensors at both inlets and outlets. Synchronized multi-view imaging of the fluorescent tracer dye and air bubbles provided visualization of the mixing phenomena. A direct comparison of the single- and multi-phase mixing coefficients showed that the fraction of leakage between the channels could be reduced by more than 80% by the addition of air bubbles to the channel flow. The integral mixing coefficients varied with the relative volumetric flux of liquid and gas. Modification of the single-phase mixing, due to the presence of the air bubbles is discussed.

## INTRODUCTION

Mixing through gaps connecting adjacent flow paths is an important mass transfer process for many thermo-hydraulic applications, such as flows through nuclear reactor rod bundles and heat exchangers. Mixing can be due to mean flows that result from pressure gradient across the gap, turbulent transport, and large-scale periodic flow structures that are produced at shear flows near

the gap/channel intersection. Several researchers have studied the fundamental flow processes occurring between parallel, gap-connected single-phase flows (Eifler and Nijsing 1967; Möller 1991, 1992; Meyer and Rehme 1994; Krauss and Meyer 1996, 1998; Baratto *et al.*, 2006; Merzari *et al.*, 2009; Mäkiharju *et al.* 2015) and multi-phase flows (Carlucci, Hammouda, & Rowe, 2004; Kawahara, Sadatomi, Kudo, & Kano, 2006; Kawahara, Sadatomi, Tomino, & Sato, 2000; van der Ros, 1970; Ylönen, 2013). Meyer (2010) offers a comprehensive review of the past work on inter-channel mixing. Single-phase inter-channel mixing has also been investigated numerically by several researchers, including Chang and Tavoularis (2006, 2007), Home *et al.* (2009), Derksen (2010), and Home & Lightstone (2014). Merzari *et al.* (2009) also used proper orthogonal decomposition to better understand the underlying dynamics of the oscillations observed in the inter-channel flow. Numerical investigation of mixing in turbulent multi-phase flows has not been extensively investigated, with results reported by Duret *et al.* (2012) and Pang (2014).

Moreover, few studies have produced single-phase, yet alone multi-phase, high Reynolds number experimental data sets that are immediately suitable for the validation of high-fidelity Computational Fluid Dynamics (CFD) models. In some reported experimental data sets, the flow inlet boundary conditions are not well characterized or uncertainties of the instruments used are not quantified. Since the resulting flows are sensitive to small changes in boundary conditions [see Ko *et al.*, (2008) for an explanation of the sensitivity of similar flows], these data are not ideally suited for rigorous CFD code Verification and Validation (V&V). Derksen (2010) performed computations of single-phase flow mixing but noted the lack of expected symmetry in the experimental data upon comparison. These results suggest that there was an underlying issue with the flow geometry, the inlet conditions, the outlet flow conditions, or some combination of these effects.

Previously reported work by Mäkiharju *et al.* (2015) examined the single phase flow mixing through narrow rectangular gaps connecting two channels with emphasis placed on defining the geometric as-built and measurement uncertainties, quantifying the inlet flow conditions. The authors closely coordinated each stage of the experiment with an accompanying CFD V&V effort to produce high-fidelity V&V data sets. The present work utilizes the same test section for the study of two-phase (water and air) mixing. The gross liquid mass transfer through the various gap openings was determined from the mass flow rate and fluorescein tracer dye concentration measurements at the channel inlets and outlets. The net air mass transfer was determined from measurements of the injected air mass fluxes and Wire-Mesh Sensor (WMS) data recorded at both the inlets and outlets. These measurements have been performed for several channel flow rate combinations at a gap height of 50 mm.

In this paper, we first describe the experimental setup, including instrumentation and measurement uncertainty. Then we discuss the multiphase mixing characteristic as compared to the single-phase flow, and we conclude with a summary and discussion future work.

## EXPERIMENTAL SETUP

This experimental investigation was conducted in a simplified canonical geometry flow facility at the University of Michigan.

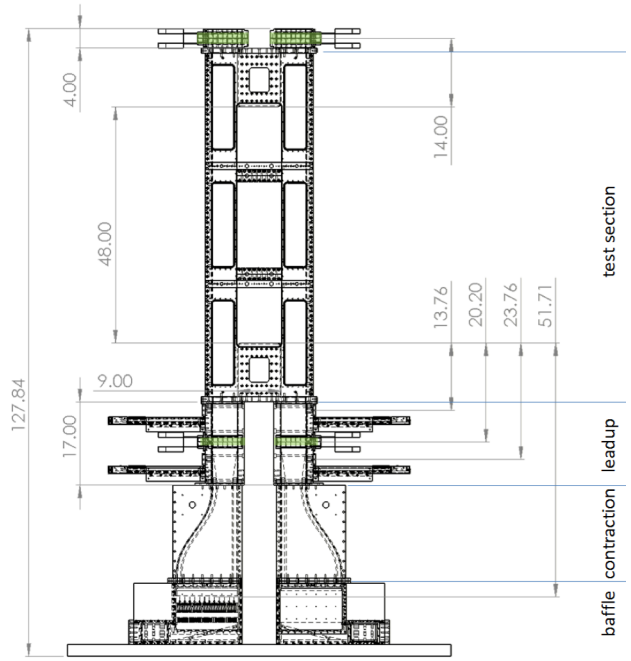


Figure 1. The geometry and dimensions of the test section. Both channels A (left) and B (right) had a hydraulic diameter, $D_h$, of 127 mm. The location of the WMS are shown in green. Dimensions shown are inches.

The vertical flow facility was constructed of an anodized aluminum frame with polished, optical grade acrylic windows to enable laser velocimetry; Particle Imaging Velocimetry; fluorescein dye and bubble tracking; and other visualization methods. Figure 1 shows a schematic drawing of the test section with key dimensions. The gap width, $W$, was 228.6 mm, length, $L$, 1219.2 mm, and the gap height, $H$, could be varied between 0 and 50 mm. The gap height for the current work was fixed to 50 ± 1 mm. Both channels had a hydraulic diameter of 127 mm and the flow surfaces had root-mean-square roughness of 1.5 μm. The channels discharged into phase separating weir tanks in which the water surface elevation was maintained at a fixed level to establish a constant back pressure at the outlets. A detailed schematic of the test section geometry is shown in Figure 2(a).

The water mass flow rates at the channel inlets were measured with Krohne Optiflux 4000 magnetic flow meters with an IFC-300C converter with a manufacturer specified accuracy ±0.2% of the reading, and at the outlets by Krohne Optimass 1400 Coriolis flow meters with a manufacturer specified accuracy ±0.24% of the reading at 5.552 x$10^{-3}$ $m^3s^{-1}$ and ±0.18% at 14.13 x$10^{-3}$ $m^3s^{-1}$. By examining flow with the gap closed and no mixing, as well as after diverting the outflow to drain and monitoring the source reservoir level, the flow meter data were found to have variability within their stated uncertainties. The absolute pressure in the test section was measured with a 0 to 207 kPa transducer (0 to 30 psia, Omega Engineering DPG409-030A) with a manufacturer specified accuracy of ±0.08% of full scale. The pressure differential across the channel inlets and outlets was measured by a differential pressure transducer with a range of -2.49 to 4.98 kPa (-10 to 20 in $H_2O$, Dwyer 3100D) and a manufacturer specified accuracy of ±0.075% of full scale. Additionally, manometers with an estimated

accuracy of ±7.5 Pa (±0.03 in $H_2O$) were also used to monitor the pressure between channels at two locations. The pressure drop from the bottom to the top of the channel was measured by a differential pressure transducer with a range of 0 to 25 kPa (0 to 100 inches of water, Rosemount 3051CD) and a manufacturer specified accuracy of ±0.04% of full scale. The water temperature was measured continuously by four 4-wire 100 ohm platinum RTD sensors (Omega Engineering P-M-A-1/4-6-0-P-3) with manufacturer specified accuracy ±(0.15 +0.002|T|) degrees C.

Water mixing through the gap was characterized by measuring fluorescein sodium salt (F6377, Sigma-Aldrich) dye concentration. A concentrated solution of fluorescein dye was injected upstream of channel B inlet pump and trace concentrations of dye were measured immediately upstream of the gap in both channels A and B. The fluorescein dye tracer was measured by a single fluorometer (Turner Designs Cyclops 7 PN 2100-000/2108-000) with a range of 0 to 500 parts per billion (ppb) and an uncertainty based on calibration defined as ±(0.5% of reading + 1 ppb). Samples for the fluorometer were automatically drawn from the channels using a valve manifold. A clean water flush was performed between each sample. Measurements in both channel exits were made far enough downstream of the gap such that the water/fluorescein sample was mixed well enough that conservation of mass for the water was achieved when measurements were made with the closed gap for high-Re flows ($8\times10^4$ and $1\times10^5$). Water/fluorescein sampling at the exit is still being investigated for low-Re flows ($4\times10^4$ and $6\times10^4$).

Each channel inlet air flow rate was set and recorded by a digital mass flow controller (Bronkhorst F-202AV-M10-AGD-55-V) with an operating range 3 to 150 slpm and a manufacturer specified accuracy ±0.5% of reading plus ±0.1% of full scale. The air was injected through two coupled 6x6 arrays of 102 (+25/-13) µm ID and 229 (+13/-0) µm OD needles and 508 (+25/-13) µm ID and 635 (+13/-0) µm OD needles in the contraction 12 hydraulic diameters upstream of the mixing gap. The outlet air fluxes were based thermal mass air flow sensor and WMS measurements. The thermal mass flow meters (Sierra 640S) were calibrated for a mass flux of 0-400 slpm and have an accuracy ±1% of reading plus ±0.5% of full scale. The WMS were manufactured by Helmholtz-Zentrum Dresden-Rossendorf (HZDR) and are based on the work by Prasser *et al.* (1998).

The present work used a conductivity based WMS system with two 48×48 meshes spaced 50 mm apart to obtain a measurement of the air void fraction, phase velocity, and bubble size distribution. Investigation of WMS performance with 100 and 200 µm diameter wire is still underway. It should be noted that smaller bubbles ($\lesssim$ 2.5 mm) tend to pass through the WMS undetected, whereas the largest bubbles ($\gtrsim$ 20 mm) cause a shadowing effect allowing smaller bubbles to pass undetected. Moreover, the authors acknowledge the intrusive nature of the WMS may affect the inflow conditions for the air-water investigation; however, these modifications from the single-phase flow were assumed to be negligible. This approach was validated by the recovery of mixing coefficient matching those previously measured by Mäkiharju *et al.* (2015). Further investigation and uncertainty quantification of the WMS instrumentation is beyond the scope of the current discussion; however, exploration of error sources and measurement quality is still being addressed. We believe that our current error approximations are reasonable for the current discussion, based on WMS error investigations by others (Beyer, Lucas, & Kussin, 2010; Ito, Prasser, Kikura, & Aritomi, 2011; Manera *et al.*, 2009; and Shaban & Tavoularis, 2016).

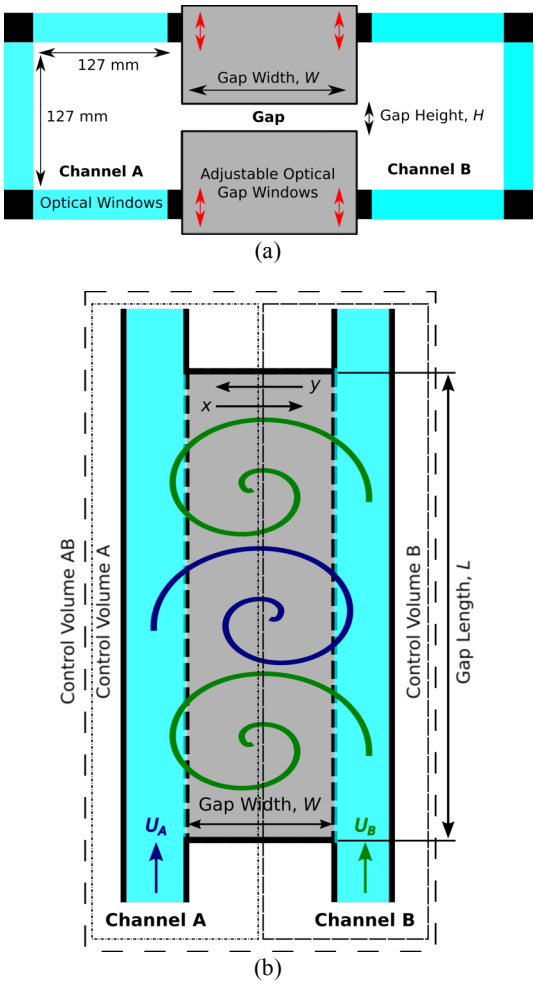


Figure 2. Schematic (not drawn to scale) section cut on center plane (a) normal (top view - flow out of the page) and (b) parallel (front view) to the primary flow direction. Large, alternating vortex structures are depicted in (b) as well.

## CHARACTERIZATION OF INTEGRAL MIXING

The mass transfer coefficients of water and air through the gap was determined assuming mass conservation for the water, air, and liquid tracer. The mixing process is schematically shown in Figure 2(b) and presented in Figure 3. The single-phase mixing for the current test geometry has been fully characterized by Mäkiharju *et al.* (2015). It was shown that, for a balanced flow between the two channels, there was no significant leakage (or gross mass transfer) for small gap heights (< 8 mm). For larger gaps, large coherent structures similar to those previously reported by others were observed. The authors described large vortex structures arising from a Kelvin-Helmholtz type instability occurred with regular temporal frequency. They also noted that the balanced flow mixing appeared to be independent of the Reynolds numbers over the parameter range investigated.

In this work we replicated the single-phase work of Mäkiharju *et al.* (2015) to measure the fluorescein dye tracer concentration, $C$, to confirm the baseline and extended the approach for the multi-

phase mixing characterization. The integral mixing coefficients denoted as $x$ and $y$ were calculated to determine the fraction of liquid leakage from channel A transferred to channel B and from channel B transferred to channel A, respectively. The mixing coefficients were determined from the conservation of mass of the water and tracer using the three test section control volumes shown in Figure 2(b). From the global control volume AB conservation of mass yields equations (1) and (2), where $\dot{m}$ is liquid mass flux.

$$\dot{m}_{A,out} + \dot{m}_{B,out} = \dot{m}_{A,in} + \dot{m}_{B,in} \quad (1)$$

$$\dot{m}_{A,out}C_{A,out} + \dot{m}_{B,out}C_{B,out} = \dot{m}_{A,in}C_{A,in} + \dot{m}_{B,in}C_{B,in} \quad (2)$$

Using the individual control volumes around channels A and B, conservation of mass provides the following four equations.

$$\dot{m}_{A,out} = \dot{m}_{A,in}(1-x) + \dot{m}_{B,in}y \quad (3)$$

$$\dot{m}_{B,out} = \dot{m}_{A,in}x + \dot{m}_{B,in}(1-y) \quad (4)$$

$$\dot{m}_{A,out}C_{A,out} = \dot{m}_{A,in}C_{A,in}(1-x) + \dot{m}_{B,in}C_{B,in}y \quad (5)$$

$$\dot{m}_{B,out}C_{B,out} = \dot{m}_{A,in}C_{A,in}x + \dot{m}_{B,in}C_{B,in}(1-y) \quad (6)$$

If the liquid volumetric flow speeds are not equal, we can derive four solutions for the mixing coefficients. For example, solving equations (3) and (5) yields $x_1$ and $y_1$, as shown in equations (7) and (8).

$$x_1 = 1 - \frac{\dot{m}_{A,out}(C_{A,out} - C_{B,in})}{\dot{m}_{A,in}(C_{A,in} - C_{B,in})} \quad (7)$$

$$y_1 = \frac{\dot{m}_{A,out}(C_{A,in} - C_{A,out})}{\dot{m}_{B,in}(C_{A,in} - C_{B,in})} \quad (8)$$

Similarly we solve for $x_2$ and $y_2$ after solving equations (4) and (6), $x_3$ and $y_3$ after solving equations (3) and (6), and $x_4$ and $y_4$ after solving equations (4) and (5). The arithmetic mean of these results $\bar{x}$ and $\bar{y}$ were used to quantify the the liquid mixing for the bubbly flow.

## EXPERIMENTAL RESULTS

Data is presented here for flow conditions at four different matched (*e.g.* balanced) inlet volumetric water flow rates of $5.0\times10^{-3}$, $7.6\times10^{-3}$, $1.0\times10^{-2}$, and $1.2\times10^{-2}$ $m^3s^{-1}$, corresponding to Reynolds numbers of $4\times10^4$, $6\times10^4$, $8\times10^4$, and $1\times10^5$. The inlet volumetric gas flow rates ranged from 0 to $3.0\times10^{-3}$ $m^3s^{-1}$. The average bubble diameter for each flow rate is presented in Table 1.

The mean mixing coefficients $x$ and $y$ at four different Reynolds numbers for the range of gas fluxes, $Q_g$ are presented in Figure 4. For the zero-gas flux, a virtually constant mixing coefficient, *i.e.*, invariable with $Re_{DH}$, of $x \approx y \approx 0.33$ is observed. Equal mass transfer from channel A to B and B to A is expected as the flow speed and geometry of both channels are nominally identical, and thus there is no mean spanwise pressure difference across the gap. As previously observed by Mäkiharju *et al.* (2015), large-scale vortices forming at the channel gap interface occurred at a nominally constant Strouhal number (0.24 to 0.25), which suggests that leakage through a narrow gap should be independent of $Re_{DH}$ (over the parameter range studied) for a specified gap height. Furthermore, equal mixing between the two channels coupled with visual observation of temporally stable vortex shedding downstream of the gap opening indicates that the Kelvin-Helmholtz type instability causing the large vortical structures is the dominant source of mixing between the two vertical channels.

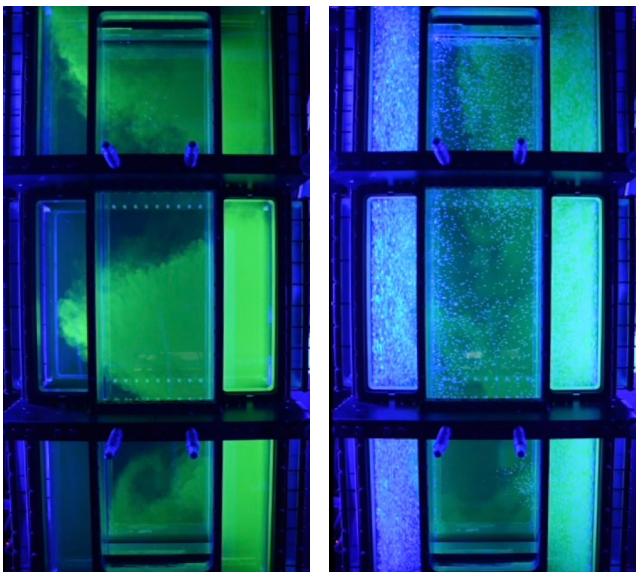

(a) (b)

Figure 3. Demonstration of mixing at $Re_{DH}$ = 60,000 with a gap height of 50 mm for (a) single-phase flow and (b) multi-phase flow with an average void fraction of approximately 4% with air injection of 20 slpm per channel. Green fluorescein dye injected upstream of the gap in channel B (right channel) provides visual evidence of the large, coherent flow structures, which dominate the liquid mass transfer between the two channels, through the narrow gap for the single-phase flow in (a). The coherent flow structures are drastically suppressed with the presence of the air bubbles, as shown in (b).

Table 1. Area-equivalent bubble diameter (mm), measured using the outlet WMS, based on nominal volumetric gas flow rate $Q_g$ and Reynolds number $Re_{DH}$.

| $Q_g$ / $Re_{DH}$ | $4\times10^4$ | $6\times10^4$ | $4\times10^4$ | $1\times10^5$ |
|---|---|---|---|---|
| 0 | 0 | 0 | 0 | 0 |
| $2.0\times10^{-4}$ | 5.1 | 4.5 | 4.6 | 4.3 |
| $4.0\times10^{-4}$ | 5.6 | 5.8 | 5.1 | 4.8 |
| $1.0\times10^{-3}$ | 7.1 | 5.5 | 5.5 | 5.2 |
| $2.0\times10^{-3}$ | 10.8 | 9.5 | 10.5 | 9.1 |
| $3.0\times10^{-3}$ | 15.4 | 11.9 | 13.2 | 13.0 |

The large vortices that shed in the gap for the single-phase flow are significantly altered as air bubbles are injected into the system. Injecting even a minimal volume of gas significantly inhibits mixing between channels A and B. By simply defining an inhibition number as the difference of the mixing coefficients with and without gas flux, normalized the single-phase mixing coefficient, *i.e.*, $I_{n,x} = \frac{x_0 - x}{x_0} = 1 - \frac{x}{x_0}$, we can quantify how the mixing is inhibited for the cases of bubbly channel flow as compared to the single-phase case. At low $Re_{DH}$, the mixing coefficients $x$ and $y$ were significantly reduced even at very small $Q_g$ of $0.17\times10^{-3}$ $m^3s^{-1}$ (10 slpm). The resulting mixing coefficients were nominally equal at 0.08, yielding an inhibition number of

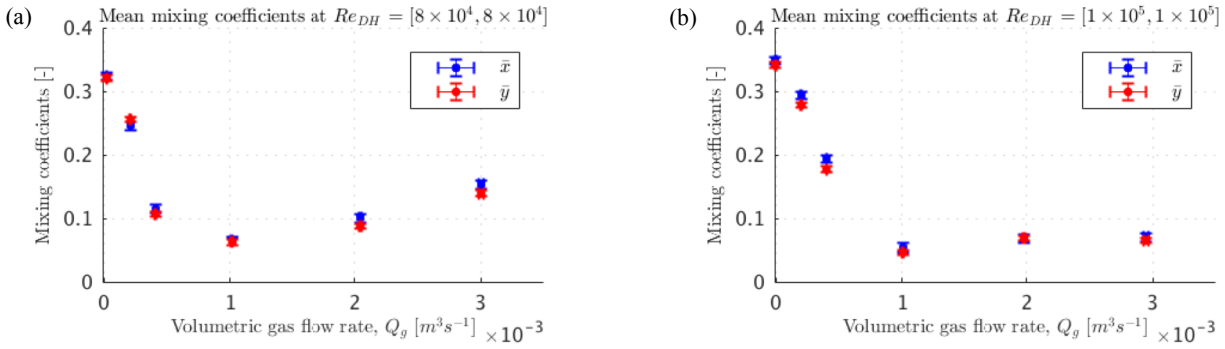


Figure 4. Mean mixing coefficients plotted against volumetric gas flow rate in at (a) $Re_{DH} = [8\times10^4, 8\times10^4]$ and (b) $Re_{DH} = [1\times10^5, 1\times10^5]$.

0.75. Further increasing the gas flux to a $Q_g$ of $0.34\times10^{-3}$ $m^3s^{-1}$ (20 slpm) further inhibits mixing at these low-$Re_{DH}$ flows, resulting in an inhibition number as large as 0.85. This flux appears to be a local minimum of liquid mixing in the lower liquid flux test cases ($Re_{DH} < 6\times10^4$). After this apparent minimum, higher gas fluxes increase the mixing coefficients; however, $I_n$ never reaches a value less than 0.40, which is the highest mixing rate for the multi-phase flow regimes tested, *i.e.*, $x \approx y \approx 0.20$. This inhibition is present for all $Re_{DH}$ tested; however, the maximum inhibition appears to vary with the gas flow rate as $Re_{DH}$ increases. That is, the mixing is minimized at higher gas flux with increasing $Re_{DH}$, up to a limit when the mixing begins to increase with an additional increase in gas flux.

The reduction in mixing was observed visually *via* the large-scale structures seen in Figure 3, which are the primary agents of mixing. From Figure 3, we see that the large-scale structures are significantly disrupted, and even fully disappear, with the addition of air bubbles to channel flow. Figure 3 clearly shows this disruptive behavior, as the distinctly moving 'S'-shaped cloud of fluorescent dye mixture has turned into an unstable two-phase flow mixture, resembling a Rayleigh-Taylor instability.

The presence of the gas seems to inhibit mixing less so at smaller gas fluxes, but more so at higher gas fluxes. At the lowest measured gas fluxes, we obtain inhibition numbers $I_{n,x}$ of only 0.18 and 0.12. When compared to the lower $Re_{DH}$ flows, the added gas flux leads to decrease in mixing. However, the location of the minima has been shifted to a higher $Q_g$. That is, for an $Re_{DH}$ of $8\times10^4$ this minimum appears to be around a $Q_g$ of $1.0\times10^{-3}$ $m^3s^{-1}$ (50 slpm). Increasing the gas flux beyond the flux which most inhibits the liquid mixing, again results in a decreased mixing inhibition or an increase in mixing. However, for an $Re_{DH}$ of $1\times10^5$ this increase in mixing from the minimum is very slight when compared to the lower Re cases, *i.e.*, $x$ only increases from 0.05 to 0.07 when the gas flux is increased by a factor of three.

At low-Re flows, there appears to be a meaningful difference between the mixing coefficients at the higher gas fluxes, suggesting more liquid mass is being transported from A to B than B to A. This imbalance in mixing increasingly diminishes at higher $Re_{DH}$, *i.e.*, the phenomenon has caused unequal leakage through gap at low $Re_{DH}$ has becomes less significant at higher flow rates. The causes of the mixing disparity, however, is currently unknown and may be the result of an unknown systematic error, or an undetected static pressure difference between the two channels.

Figure 5 shows the average mixing coefficients, $[\bar{X} = 1/2(\bar{x} + \bar{y})]$, mostly collapse with the volumetric quality, $\beta = Q_g/(Q_g + Q_l)$, which demonstrates the mixing depends on the volumetric ratio of gas to liquid flux. The average of the mixing coefficients drastically decreases from 0.33 to 0.05 for $\beta$ of zero to 0.05, after which mixing begins to increase with increasing $\beta$. The reason for this local minimum is still being investigated and is currently being explored for additional gap heights. At first glance, inhibited mixing occurs due to a breakdown of the naturally occurring Kelvin-Helmholtz type instability that causes large, coherent structures in the absence of bubbles. This argument is supported by Yoon's (2017) recent investigation of the proper orthogonal decomposition (POD) of the mixing modes for single-phase mixing.

## CONCLUSIONS

Injection of nominally monodispersed air bubbles into adjacent, vertical flow channels connect by a narrow gap has been shown to drastically decrease the liquid mixing and mass transfer between the channels. The amount by which mixing is inhibited depends on the combination of injected gas flux and the Reynolds number. The main mechanism of reducing the mixing appears to be inhibiting the formation of the large coherent structures previously observed. Indications of preferred mixing conditions have been found using the measurements performed. Mixing was shown to collapse across a range of Reynolds numbers with respect to the volumetric quality, or the ratio of gas and liquid in the system. Visual observations that bubbles are being convected between the channels along with the water due to their entrainment in the vortices were reviewed, and will be explored further to aid in the understanding of the reduced mixing for multi-phase flows as compared to the single-phase flows.

As indicated by the data gathered thus far, the introduction of gas inhibits the natural development of the Kelvin-Helmholtz type instability. The reduction in mixing coefficient appears to correlate with loss of contribution to mixing by the large, coherent structures represented by the first mode(s) of the POD analysis for the single-phase mixing (Yoon 2017). A more detailed analysis of the mixing modes, supported by additional data, is underway.

Additionally, the authors are further exploring the parameter space, including varying gap heights and flow rates, to further develop the physical understanding of the multi-phase mixing phenomenon. Acquisition of additional data, analysis or the results, and accompanying CFD effort, and more detailed comparison between the experimental and CFD data are ongoing.

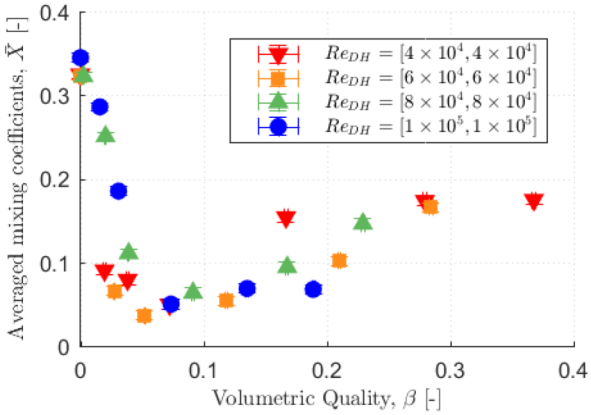


Figure 5. Average mixing coefficients were shown to vary with the volumetric quality of the inlet mixture. The results are insensitive to changes in the channel Reynolds number.

## REFERENCES


Baratto, F., Bailey, S. C. C., & Tavoularis, S. 2006. Measurements of frequencies and spatial correlations of coherent structures in rod bundle flows. Nuclear Engineering and Design, 236, 1830–1837.

Beyer, M., Lucas, D., & Kussin, J. 2010. Quality check of wire-mesh sensor measurements in a vertical air/water flow. Flow Measurement and Instrumentation, 21, 511–520.

Carlucci, L. N., Hammouda, N., & Rowe, D. S. 2004. Two-phase turbulent mixing and buoyancy drift in rod bundles. Nuclear Engineering and Design, 227, 65–84.

Chang, D., & Tavoularis, S. 2006. Convective Heat Transfer in Turbulent Flow Near a Gap. Journal of Heat Transfer, 128, 701.

Chang, D., & Tavoularis, S. 2007. Numerical simulation of turbulent flow in a 37-rod bundle. Nuclear Engineering and Design, 237, 575–590.

Derksen, J. J. 2010. Simulations of lateral mixing in cross-channel flow. Computers and Fluids, 39, 1058–1069.

Duret, B., Luret, G., Reveillon, J., Menard, T., Berlemont, A., & Demoulin, F. X. 2012. DNS analysis of turbulent mixing in two-phase flows. International Journal of Multiphase Flow, 40, 93–105.

Eifler, W., & Nijsing, R. 1967. Experimental investigation of velocity distribution and flow resistance in a triangular array of parallel rods. Nuclear Engineering and Design, 5, 22–42.

Home, D., Arvanitis, G., Lightstone, M. F., & Hamed, M. S. 2009. Simulation of flow pulsations in a twin rectangular sub-channel geometry using unsteady Reynolds Averaged Navier-Stokes modelling. In Nuclear Engineering and Design (Vol. 239, pp. 2964–2980).

Home, D., & Lightstone, M. F. 2014. Numerical investigation of quasi-periodic flow and vortex structure in a twin rectangular subchannel geometry using detached eddy simulation. Nuclear Engineering and Design, 270, 1–20.

Ito, D., Prasser, H. M., Kikura, H., & Aritomi, M. 2011. Uncertainty and intrusiveness of three-layer wire-mesh sensor. Flow Measurement and Instrumentation, 22, 249–256.

Kawahara, A., Sadatomi, M., Kudo, H., & Kano, K. 2006. Single- and Two-Phase Turbulent Mixing Rate between Subchannels in Triangle Tight Lattice Rod Bundle. JSME International Journal Series B, 49, 287–295.

Kawahara, A., Sadatomi, M., Tomino, T., & Sato, Y. 2000. Prediction of turbulent mixing rates of both gas and liquid phases between adjacent subchannels in a two-phase slug-churn flow. Nuclear Engineering and Design, 202, 27–38.

Ko, J., Lucor, D., & Sagaut, P. 2008. Sensitivity of two-dimensional spatially developing mixing layers with respect to uncertain inflow conditions. Physics of Fluids, 20. doi:10.1063/1.2937465

Krauss, T., & Meyer, L. 1996. Characteristics of turbulent velocity and temperature in a wall channel of a heated rod bundle. Experimental Thermal and Fluid Science, 12, 75–86.

Krauss, T., & Meyer, L. 1998. Experimental investigation of turbulent transport of momentum and energy in a heated rod bundle. Nuclear Engineering and Design, 180, 185–206.

Mäkiharju, S. A., Ceccio, S. L., Buchanan, J. R., Mychkovsky, A. G., Hogan, K. J., & Lowe, K. T. 2015. Experimental Characterization of Interchannel Mixing Through a Narrow Gap. In International Topical Meeting on Nuclear Reactor Thermal Hydraulics 2015, NURETH 2015 (Vol. 5, pp. 4394–4409).

Manera, A., Ozar, B., Paranjape, S., Ishii, M., & Prasser, H.-M. 2009. Comparison Between Wire- Mesh Sensors and Conductive Needle- Probes for Measurements of Two- Phase Flow Parameters. Nuclear Engineering and Design, 239, 1718–1724.

Merzari, E., Ninokata, H., Mahmood, A., & Rohde, M. 2009. Proper orthogonal decomposition of the flow in geometries containing a narrow gap. Theoretical and Computational Fluid Dynamics, 23, 333–351.

Meyer, L. 2010. From discovery to recognition of periodic large scale vortices in rod bundles as source of natural mixing between subchannels-A review. Nuclear Engineering and Design, 240, 1575–1588.

Meyer, L., & Rehme, K. 1994. Large-scale turbulence phenomena in compound rectangular channels. Experimental Thermal and Fluid Science, 8, 286–304.

Möller, S. V. 1991. On phenomena of turbulent flow through rod bundles. Experimental Thermal and Fluid Science, 4, 25–35.

Möller, S. V. 1992. Single-phase turbulent mixing in rod bundles. Experimental Thermal and Fluid Science, 5, 26–33.

Pang, B. 2014. Numerical study of void drift in rod bundle with subchannel and CFD codes. doi:10.5445/KSP/1000041053

Shaban, H., & Tavoularis, S. 2016. On the accuracy of gas flow rate measurements in gas – liquid pipe flows by cross-correlating dual wire-mesh sensor signals. International Journal of Multiphase Flow, 78, 70–74.

van der Ros, T. 1970. On two-phase flow exchange between interconnected hydraulic channels. Technische Hogeschool Eindhoven.

Ylönen, A. 2013. High-resolution flow structure measurements in a rod bundle, PhD Diss, Lappeenranta University of Technology.

Yoon, S. 2017. Electron Beam X-Ray Computed Tomography for Multiphase Flows and An Experimental Study of Inter-channel Mixing. PhD Diss., University of Michigan.